

Final Report to  
NASA Advanced Design Program Office  
for Contract NAGW-4337

***Integrated Design and Manufacturing for the  
High Speed Civil Transport***  
(A combined Aerodynamics/Propulsion Optimization Study)

Student Design Team

*Juergen Baecher  
Oliver Bandte  
Dan DeLaurentis  
Kemper Lewis  
Jose Sicilia  
Craig Soboleski*

Faculty Advisors

*Dr. Daniel P. Schrage  
Principal Investigator  
Professor & Co-Director (ASDL)*

*Dr. Dimitri N. Mavris  
Assistant Professor & Associate Director (ASDL)*

*December 16, 1995*

*Aerospace Systems Design Laboratory (ASDL)  
School of Aerospace Engineering  
Georgia Institute of Technology  
Atlanta, GA 30332-0150*

## **Foreword**

This report documents work completed during Georgia Tech's third year of involvement with NASA's Advanced Design Program (ADP). The work herein was performed by the student team members under the advisement and coordination of Dr. Dan Schrage and Dr. Dimitri Mavris, Co-Director and Associate Director of the Aerospace Systems Design Laboratory (ASDL) in the School of Aerospace Engineering, respectively. The design team would like to take this opportunity to thank the following individuals for their valuable assistance: Florian Bachmaier, Andreas Hahn, Jae Moon Lee, Peter Rohl, Jimmy Tai, Bill Marx, and Jason Brewer.

The following individuals comprised the 1995 Georgia Tech ADP Design Team. Listed with their names are the areas in which they were responsible for in the study. The team leader was Dan DeLaurentis.

Juergen Baecher  
Oliver Bandte  
Dan DeLaurentis  
Kemper Lewis  
Jason Pratt  
Jose Sicilia  
Craig Soboleski

Aerodynamics, Shell Scripts  
Response Surface Modeling  
Synthesis/Sizing  
Propulsion  
Propulsion, Manufacturing  
Propulsion, Sizing  
FLOPS Modifications

## Executive Summary

This report documents the efforts of a Georgia Tech HSCT Aerospace Student Design Team in completing a design methodology demonstration under NASA's Advanced Design Program (ADP). Aerodynamic and Propulsion analyses are integrated into the synthesis code FLOPS in order to improve its prediction accuracy. Executing the Integrated Product and Process Development (IPPD) methodology proposed at the Aerospace Systems Design Laboratory (ASDL), this report describes an improved sizing process followed by a combined aero-propulsion optimization, where the objective function, average yield per Revenue Passenger Mile (\$/RPM), is constrained by flight stability, noise, approach speed, and field length restrictions. Primary goals for the team included successful demonstration of the application of RSM to parameter design, introduction of higher fidelity disciplinary analysis than normally feasible at the conceptual and early preliminary level, and, in sum, investigation of relationships between aerodynamic and propulsion design parameters and their effect on the objective function, \$/RPM.

This report develops a unique approach to aircraft synthesis in which statistical methods, specifically Design of Experiments and the Response Surface Methodology, are used to more efficiently search the design space for optimum configurations. In particular, two uses of these techniques will be demonstrated. First, response model equations will be formed which represent complex analysis in the form of a regression polynomial. Next, a second regression equation will be constructed, not for modeling purposes, but instead for the purpose of optimization at the system level. Such an optimization problem with the given tools normally would be difficult due to the need for hard connections between the various complex codes involved. The methodology put forward in this report presents an alternative using the above mentioned statistical approach, and is demonstrated via an example of aerodynamic modeling and planform optimization for a High Speed Civil Transport aircraft.

## I. Introduction

Over the past few years, much research has taken place on the topic of how best to design complex aerospace systems. Much of this effort has been conducted under the general term of Multidisciplinary Design Optimization (MDO). MDO has been defined as "A methodology for the design of complex engineering systems that are governed by mutually interacting physical phenomena and made up of distinct interacting subsystems".<sup>1</sup> One of the earliest and most well known approaches to executing MDO was through the Global Sensitivity Equations approach, where "what if" questions are answered through so-called system sensitivity derivatives which relate a system response to changes in design variables, including the interactions of the disciplines involved. Examples are seen in References 2 and 3, though there are numerous others. The strength of the GSE lies in the determination of interactions between disciplines in a structured and logical manner. These interactions, represented as sensitivities, can then be used as gradient information in a traditional optimization exercise. The GSE approach, though, provides only local gradient information and some of the derivatives may be difficult to calculate. Malone and Mason have used the GSE approach in combination/coordination with other techniques and tools in an attempt to improve on some of the shortcomings and give more insight to the designer.<sup>4</sup> However, for vehicle synthesis (a truly multidisciplinary problem), with numerous interacting disciplines, many design variables (both continuous and discrete), and often times relatively inaccurate contributing analysis, an effective and comprehensive methodology has not emerged.

This report describes some new developments which form the initial execution of an evolving Integrated Product and Process Design (IPPD) approach. Traditional sizing is performed with somewhat rudimentary tools due to the impracticability of connecting complex codes together into an iterative sizing code. The use of statistical techniques in the proposed method allows for more flexibility in searching a design space by representing large amounts of knowledge (e.g. complex, expensive analysis codes or physical experiments) via response surface equations (RSEs). Caveats in the use of statistical approximations in the replacement of complex analysis

include accuracy and scope issues. How well the fitted equations represent the given data will be important in determining the validity of the results. Also, the RSEs are valid only in the design space (multidimensional region bounded by the range extremes for each design variable considered) for which they were formed. Thus, they will only produce designs which are "conventional" in so far as conventional is defined by the size of the design space chosen. These issues will be revisited throughout the remainder of this report.

The approach put forward in this study addresses a multidisciplinary problem (the synthesis of an aircraft) from an Integrated Product and Process Design (IPPD) perspective, where the recomposition portion of the synthesis is executed using Design of Experiments (DOE) and the above mentioned RSEs. These techniques allow for the introduction of more accurate contributing analysis into the synthesis and sizing process. RSEs have been used in the aerospace field over the past several years by several groups.<sup>5,6</sup> A key development presented here, however, is that a systematic plan for incorporating RSEs directly into a vehicle synthesis code as "model" equations has been developed. This process is demonstrated by modeling the mission aerodynamics (i.e. vehicle drag as a function of planform shape, overall geometry, and flight condition) via RSEs, incorporating these RSEs into a synthesis code, and then using this modified code to conduct a system rather than discipline level optimization. The key objective at the system level is *affordability*.

## II. IPPD Approach to System Recomposition

The Georgia Tech IPPD methodology can best be viewed as a recomposition process, employed once the various parts of the problem have been broken down and analyzed. In order to do this recomposition in a meaningful way, *Product* and *Process* design variables and constraints must be considered simultaneously. Product characteristics are those that pertain directly to the subject of product design, such as geometry, materials, propulsion systems, etc. Process characteristics, on the other hand, refer to those items related to how the product is designed, produced, and sustained over its lifetime. A rational approach to executing the integration process takes the form of a "Funnel", as illustrated in Figure 1.

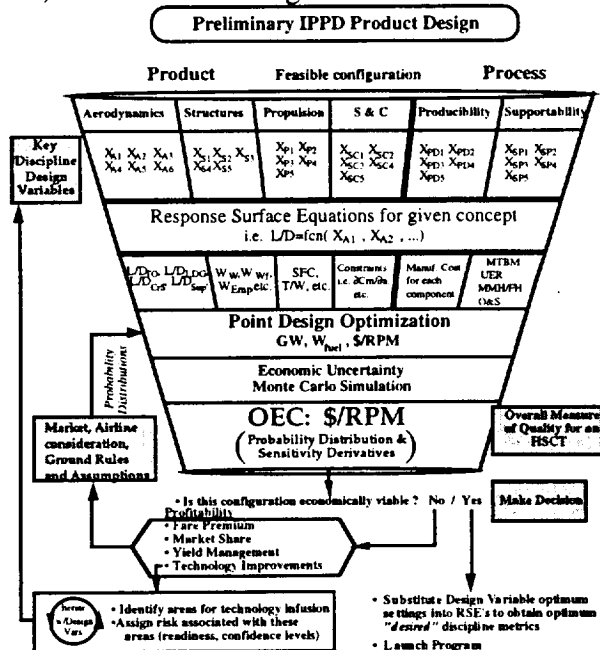


Figure 1: Systematic Recomposition

In essence, the Funnel represents a concurrent recomposition process in which all of the various disciplinary interactions, ideally, are accounted for during "synthesis", or recomposition.

In reality, as this is a developing methodology, smaller parts are tackled first in order to discover the strengths and weaknesses of the method. For this study, the aerodynamic and propulsion disciplines were examined in detail, with stability and control introduced as constraints, and structures considerations being limited to component weight estimation based on historical data compiled in the sizing code FLOPS (FLight OPTimization System). The first level in the funnel represents fundamental design variables in each category. These are the parameters available to the engineer in formulating configurations. The next step, the introduction of RSM, is the newest innovation in the approach, and its importance lies in two facts. First, it allows the formation of response equations which can be used to replace complex simulation codes needed to arrive at a point design optimum. Second, as is illustrated at the bottom of the figure, once economically viable alternatives are synthesized, these RSEs can be used to obtain the *discipline metrics*, such as L/D or SFC, which correspond to the optimal configuration. After the equations are formed, this discipline level information is used to perform system synthesis (with appropriate constraints) through the use of FLOPS. What is thus obtained are the various design variable settings which correspond to the point design optimum (i.e. one aircraft configuration) and a corresponding \$/RPM value. The \$/RPM (dollars per Revenue Passenger Mile) is the selected Overall Evaluation Criterion (OEC) for commercial aircraft. The \$/RPM represents the ticket price, on a per mile basis, that an airline must charge in order to achieve a specified return on investment (ROI) for itself and the manufacturer of the aircraft. Unfortunately, this optimal result for the OEC can never be achieved exactly due economic factors of which the designer cannot control, such as market and airline considerations. These economic factors introduce a distribution for \$/RPM that subsequently is used to determine if economic viability has been achieved (based on the needs of the airline and manufacturer) or if a design iteration (see bottom, right of figure) is necessary.

The need for disciplinary approximations becomes evident in Figure 1, as the connection of complicated analysis tools (e.g. CFD for aerodynamics, FEM for structures, cycle analysis for propulsion, etc.) from each discipline would be impractical. Common design variables, if they exist, between areas can be represented as noise factors in the formation of particular RSEs. For example, the position of the engine nacelles, a decision made by the propulsion and stability person, is kept as a variable in the aerodynamic model equation formation.

### **III. Design of Experiments and the Response Surface Method**

Understanding the characteristics of the design space and behavior of the proposed designs as efficiently as possible is as important to the designer as finding the numerical optimum. This is particularly true for complex aerospace systems which require multidisciplinary analyses, a large investment of computing resources, and intelligent data management. Although automated iterative optimization programs are useful (in that they are readily applied to engineering design in general), their drawbacks include an inability to exploit domain knowledge and high sensitivity to the manner in which a problem is formulated. In addition, due to the iterative nature, a significant amount of information is used merely in an intermediate step in the iteration process and is lost when the optimization run is finished.

The Response Surface Methodology (RSM) comprises a group of statistical techniques for empirical model building and exploitation. By careful design and analysis of experiments, it seeks to relate a response, or output variable, to the levels of a number of predictors, or input variables. In most cases, the behavior of a measured or computed response is governed by certain laws which can be approximated by a deterministic relationship between the response and a set of design variables; thus, it should be possible to determine the best conditions (levels) of the factors to optimize a desired output<sup>8</sup>. Unfortunately, many times the relationship between response and predictors is either too complex to determine or unknown, and an empirical approach is necessary to determine the behavior. The strategy employed in such an approach is the basis of the RSM. In this current application, a second degree model of the selected responses in  $k$ -variables is assumed to exist. A notional example of a second order model is displayed in Figure 2 for two variables  $x_1$  and  $x_2$ .

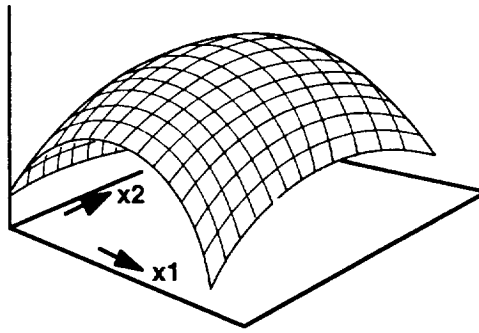


**Figure 2: Second Order Response Surface Model**

The second degree RSE takes the form of:

$$R = b_0 + \sum_{i=1}^k b_i x_i + \sum_{i=1}^k b_{ii} x_i^2 + \sum_{i < j}^k b_{ij} x_i x_j \quad (1)$$

where,  $b_i$  are regression coefficients for the first degree terms,  $b_{ii}$  are coefficients for the pure quadratic terms,  $b_{ij}$  are coefficients for the cross-product terms (second order interactions), and  $b_0$  is the intercept term. To facilitate the discussion to follow, the components of equation (1) are further defined. The  $x_i$  terms are the “main effects”, the  $x_i^2$  terms are the “quadratic effects”, and the  $x_i x_j$  are the “second-order interaction terms”.

Once this equation is constructed from the sample data through a least squares technique, it can be used in lieu of more sophisticated, time consuming computations to predict and/or optimize the response  $R$ . If one is optimizing on  $R$ , the “optimal” settings for the design variables are identified (through any number of techniques) and a confirmation case is run using the actual simulation code to verify the results. Since the RSE is in essence a regression curve, a series of experimental or computer simulation runs must be performed to obtain a set of data for regression. One organized way of obtaining these data is the aforementioned DOE, which is used to determine a table of input variables and combinations of their levels yielding a response value (but also encompasses other procedures, like Analysis of Variance). There are many types of DOEs. Table 1 displays a simple full factorial example for three variables at two levels, a minimum and a maximum (sometimes also described as “-1” and “+1” points). The response can be any of a variety of metrics (such as thrust, drag, pitching moment, weight, etc.), while the design variables (or control factors) define the design space. For the approach in this report, the factors become input variables to the analysis code, while the response is generally the desired output of the program.

**Table 1: Design of Experiment Example for a two-level,  $2^3$  Factorial Design<sup>9</sup>**

| Run | Factors |   |   | Response |
|-----|---------|---|---|----------|
|     | 1       | 2 | 3 |          |
| 1   | -       | - | - | $y_1$    |
| 2   | +       | - | - | $y_2$    |
| 3   | -       | + | - | $y_3$    |
| 4   | +       | + | - | $y_4$    |
| 5   | -       | - | + | $y_5$    |
| 6   | +       | - | + | $y_6$    |
| 7   | -       | + | + | $y_7$    |
| 8   | +       | + | + | $y_8$    |

A statistical analysis can be performed using Analysis of Variance (ANOVA) with t-Tests in estimating the model parameters for the RSE. The same DOE approach can be used for

variables at three levels, requiring more runs to obtain the same information. On the other hand, evaluation of all possible combinations of variables at two or three levels increases the number of cases that need to be tested exponentially, and thus is not practical. In fact, testing these variables at three levels, their two extremes and a center point, would take a total of 531,441 cases for a  $3^{12}$  factorial design. Table 2 illustrates that one way of decreasing the number of experiments or simulation runs required is to reduce the number of variables. But as Table 2 also displays, a  $3^7$  full factorial design requires 2,187 runs, which is still considered impractical for experiments or computer simulations. Hence, fractional factorial and second order model designs (of which the Central Composite is an example) are proposed as a more plausible means to perform experiments. Table 2 provides three examples.

**Table 2: Number of Cases Required for Different DOEs<sup>9</sup>**

| DOE                            | 7 Variables | 12 Variables | Equation       |
|--------------------------------|-------------|--------------|----------------|
| <b>3-level, Full Factorial</b> | 2,187       | 531,441      | $3^n$          |
| <b>Central Composite</b>       | 143         | 4,121        | $2^n + 2n + 1$ |
| <b>Box Behnken</b>             | 62          | 2,187        | -              |
| <b>D-Optimal Design</b>        | 36          | 91           | $(n+1)(n+2)/2$ |

Fractional factorial DOEs use less information to come up with results similar to full factorial designs. This is accomplished by reducing the model to only account for parameters of interest. Therefore, fractional factorial designs often neglect third or higher order interactions for an analysis (see RSE in Equation (1)), accounting only for main and quadratic effects and second order interactions. Thus, the model used in this report neglects third and higher order interactions and a tradeoff exists in fractional factorial designs. The number of experiments or simulations (often referred to as "cases") rises as the increasing degree to which interaction and/or high order effects are desired to be estimated. Practically, since generally only a fraction of the full factorial design number of cases can be run, high order effects and interactions are not estimable. They are said to be confounded, or indistinguishable, from each other in terms of their effect on the response. This aspect of fractional factorial designs is described by the *resolution*. Resolution III implies that main effects are confounded with second order interactions. Thus, one must assume these interactions to be zero in order to estimate the main effects. Resolution IV indicates that all main effects are estimable, though second order interactions are confounded with other such interactions. Resolution V or greater means that both main effects and second order interactions are estimable (though for Resolution V designs, third order interactions would be confounded with second order effects, hence must be zero)<sup>10</sup>. The example presented in Section IV will employ a Resolution V design for the generation of RSEs. Another possibility for reducing the number of cases is to give up the ability of accounting for replicates. Replicates are normally used to provide for the calculation of experimental error (as opposed to model fit error). Since we assume that our computer simulations are "exact" or repeatable, replicates are not needed for this application of DOE.

As a general approach, a first DOE is performed in order to reduce the number of variables by identifying the contribution to the response of each variable considered. This exercise, termed a screening test, uses a two level fractional DOE for testing a linear model, thus estimating the main effects of the design variables on the response. It allows for an investigation of a high number of variables to gain a first understanding of the problem and the design space. A visual way to see the results of this screening is through a Pareto Chart<sup>11</sup>, displayed in Figure 3. It identifies in a bar chart the most significant contributors to the response based on the linear equation generated from the DOE data. A line of cumulative contribution indicates which variables contribute how much.

By defining the percentage of contribution desired, the number of variables needed to be carried along can be determined from the array of variables in the Pareto Chart. Usually, 7 to 8 variables are selected from the Pareto Chart to be carried over to the next step of generating the Response Surface Equation.

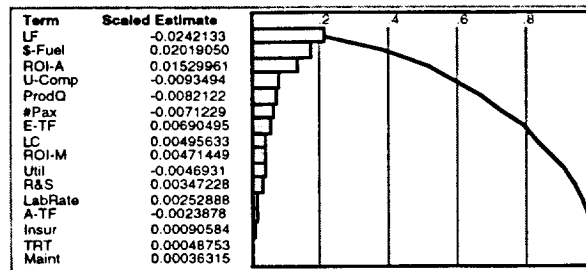


**Figure 3: Pareto Plot - Effect of Design Variables on the Response**

Figure 4 illustrates for a simple two variable case the two steps of this approach and the different shapes of the response function. The two level, linear model of  $y$  as a function of  $x_1$  and  $x_2$  represents the screening test. Here it is seen that response  $y$  is not highly dependent on  $x_1$ . With this information, the actual generation of an RSE takes place only with  $x_2$  but in a quadratic model setting. By reducing the number of variables considered, the order of effects estimable in the RSE is increased. The payoff, of course, is for cases for numerous variables. Unfortunately, the process can be depicted visually only for the simple two variable case.

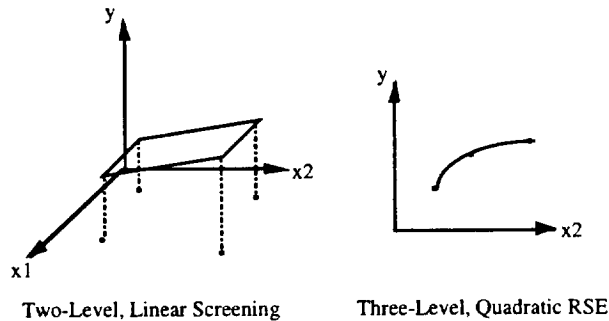


**Figure 4: Two Steps Towards Response Surface Equations**

After identifying the variables to be carried through to an RSE, a particular type of DOE must be selected. For the purposes of this study, the Central Composite Design (CCD)(Figure 5) was selected to form the RSE. The particular CCD chosen is a five level composite design formed by combining a two level full or fractional factorial design with a set of axial or star and center points as described in References 8 and 12. It is an economical design in terms of the number of runs required, as Figure 5 illustrates by displaying a design for three variables as a cube with star and center points. The distance between axial points describes the extents of the design space. The points on the corners of the cube, on the axis, and in the center of the cube are additionally examined points as identified by the DOE scheme of levels for each variable. The center provides multiple replicates, for estimating experimental error, which is assumed non-existent for simulation-based analysis. Hence, just one replicate is required for the center point.



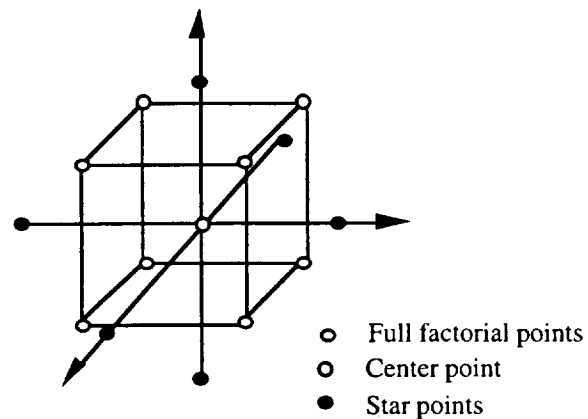


**Figure 5: Central Composite Design Illustration for Three Variables**

Finally, with the Central Composite Design in hand, an RSE can be obtained by using Equation (1) as a model for regression on the generated data. Unlike for true experiments, a statistical environment without any error can be assumed, so that all deviations from the predicted values are true measures of a model fit. A lack of fit parameter for the model expresses how good the model represents the true response. A small lack of fit parameter usually indicates existing higher order interactions not accounted for in the model. Depending on the level of this lack of fit, a new design with a transformed model to account for these interactions should be used.

#### **IV. Example: Aero-Propulsion Optimization for an HSCT**

The methodology described above is best understood via a detailed execution example. This example, the synthesis and optimization of a High Speed Civil Transport, is developed in the rest of this report. Choosing a planform shape for a supersonic transport is a task that to this day is still a long and tedious one. The need for efficient performance at both sub- and supersonic cruise conditions exhibit immediately the presence of conflicting design objectives. Studies by Boeing and Lockheed during the 1970's for the SuperSonic Transport (SST) program looked extensively at this issue<sup>13,14</sup>. Basically what emerged was that low aspect ratio, highly swept wings have low drag at  $M > 1$ , since the cranked leading edge serves to provide subsonic type flow normal to the wing leading edge. Unfortunately, such planforms are poor in subsonic cruise. Another option studied was the variable sweep wing, which, as the name implies, has the advantage of adapting to the flight condition. However, complications involving reduced fuel volume and weight and complexity penalties resulted in this concept never being seriously considered. The so-called double delta emerged as a compromise. Here the outboard panel helps retain some subsonic performance while keeping acceptable supersonic cruise efficiency<sup>13</sup>. The study carried out presently employs a DOE technique which models and examines planforms ranging from the pure delta (arrow) to the double delta.

The trades involved in planform selection are complicated by the presence of design and performance constraints at the system level which are directly related to the wing. The limit on approach speed, for example, is mostly a function of wing loading. Similarly, fuel volume requirements impact the wing size since most of the fuel is carried in tanks located inside the wing structure. Both of these issues become sizing criteria and both tend to increase the wing in size. Of course, increased wing area brings with it higher induced and skin friction drag. Terminal performance at takeoff and landing (especially field length limitations) also presents a challenge. Increasing the low speed aerodynamic performance of the aircraft will reap benefits for noise control through reduced thrust and more modest climb rates. The HSCT will need its maximum  $C_L$  at takeoff, and the use of high lift devices will play a major role in making that maximum as high as possible. Based on typical data from the SST studies, a configuration of flap settings was selected for the baseline aircraft in this example and the takeoff and landing polars were generated using the code AERO2S<sup>15</sup>.

## A. Problem Formulation

The problem consists of using the new techniques outlined in Sections II and III in synthesizing and eventually optimizing an HSCT type aircraft for a given mission. Improved aerodynamic procedures over what is currently available in the synthesis code FLOPS are incorporated via RSEs. Finally, an RSE for the overall objective function (\$/RPM) and several performance constraints are generated and a constrained optimal solution (using aerodynamic and propulsion design variables) is found.

## B. Forming RSEs for Mission Drag

The goal of introducing RSEs is to replace the existing drag calculation in the synthesis code FLOPS. Ordinarily FLOPS determines drag at a certain flight condition (i.e. Mach number and altitude) by one of three methods: internal calculations (based on the EDET aero prediction program<sup>16</sup>), externally generated drag table, externally generated polar equation. Considering the functional form of the drag polar equation:

$$C_D = C_{D0} + k_2 \cdot C_L^2 \quad (2)$$

RSEs for  $C_{D0}$  and  $k_2$ , are to be formed as a function of design variables and operational Mach number. Thus, the total drag for a given aircraft configuration will again be a function of Mach number and  $C_L$  as well as design variables. The first step in forming the response model equations is to first conduct a screening test. Even with the computational advantages brought by DOE, an excessive number of design variables can make the RSE generation expensive/difficult (See Table 2). The design variables which are to make up the RSE model for vehicle drag must be the ones which have the most influence on the aerodynamic characteristics of the airplane and, perhaps most importantly, that the designer could control. A screening test is designed to identify the subset of design variables which contribute most to a given response (i.e. the variables for which the response has the highest sensitivity). To begin the screening process, a parametric wing planform definition scheme must be selected which encompasses the variety of wing shapes considered for a supersonic transport: from a pure arrow wing to a kinked double delta. This excludes, for example, fuselage length and diameter since these are given by the number of passengers to be carried. A summary of all the design variables selected can be found in Figure 6.

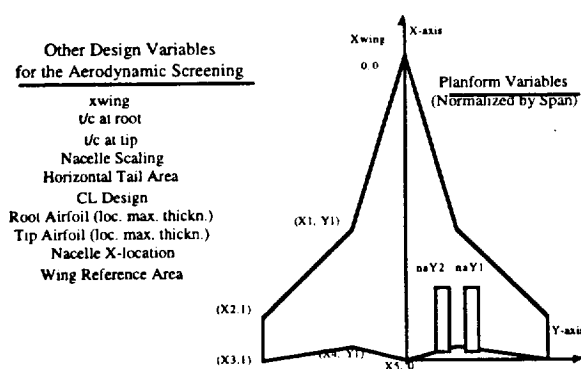


**Figure 6: Aerodynamic Design Variable Selection**

Choosing meaningful ranges for the design variables is critical. On the one hand, the ranges should be somewhat large to include the largest design space possible and increase the chances that the eventual optimal configuration is captured. On the other hand, the range must not be chosen so large as to reduce the prospects of a good fit of the RSE (second order polynomials in this example) to the actual highly non-linear response.

Additionally, there are physical restrictions which limit the range choices. For example, the wing at its aftmost location with longest root chord must not interfere with the horizontal tail. Table 3 shows a summary of all design variables with their chosen ranges. Recall that planform variables are normalized by span, selected based on review of past and present concepts, and that the screening test is a 2-level (or linear) test. Since we are not interested in forming an equation just yet, the linear sensitivities are expected to do just as well in determining which are the most important contributors. A sampling of some shapes investigated is shown in Figure 7.

**Table 3: Ranges for Aerodynamic Design Variables**

| Variable                           | Symbols | Lower Bound | Upper Bound |
|------------------------------------|---------|-------------|-------------|
| Kink X-loc.                        | X1      | 1.54        | 1.69        |
| Tiploc leading edge                | X2      | 2.10        | 2.36        |
| Tiploc trailing edge               | X3      | 2.40        | 2.58        |
| Kinkloc trailing edge              | X4      | 2.19        | 2.36        |
| Kink Y-loc.                        | Y1      | 0.44        | 0.58        |
| Root Chord                         | X5      | 2.19        | 2.50        |
| Nacelle (1) Y-loc.                 | NAY1    | 0.25        | 0.35        |
| Nacelle (2) Y-loc.                 | NAY2    | 0.45        | 0.55        |
| Nacelle X-loc.                     | NAX     | 10.30       | 16.50       |
| Wing Area                          | S       | 8500.00     | 2500.00     |
| X-loc. of Wing                     | XWING   | 0.25        | 0.33        |
| t/c Root                           | TCI     | 2.70        | 3.30        |
| t/c Tip                            | TCO     | 2.30        | 2.80        |
| Nacelle Scaling                    | NAC     | 1.00        | 1.20        |
| Area of Hor. Tail                  | STAIL   | 400.00      | 750.00      |
| CL Design                          | CLDES   | 0.08        | 0.12        |
| Root Airfoil (loc. max. thickness) | IAF     | 0.50        | 0.60        |

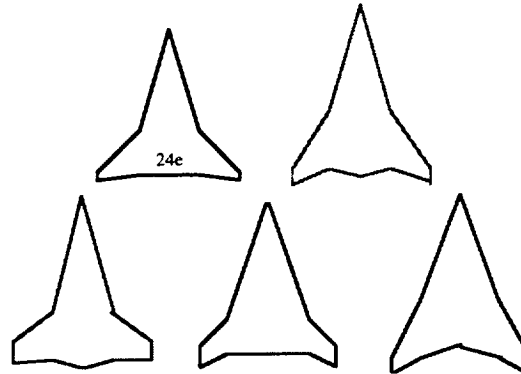


**Figure 7: Variety of Planform Possibilities for HSCT Example**

Two 2-level experiments are conducted, one each for the two selected responses ( $C_{D0}$ ,  $k_2$ ) and the results are visually inspected via the aforementioned Pareto Chart, an example of which appears in Figure 8 for the  $M=2.4$  case as an example.

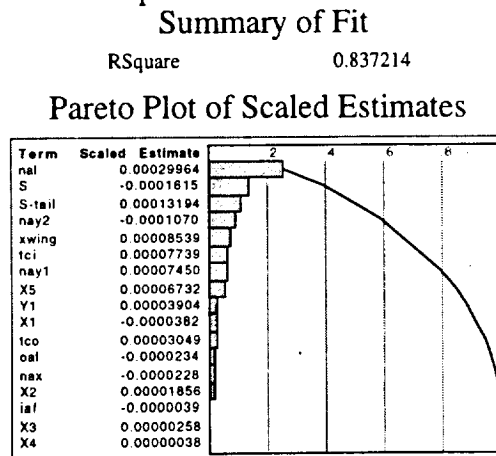


**Figure 8: Screening of Aerodynamic Variables for  $C_{D0}$ , Mach 2.4**

As explained in Section III, the important information in the Pareto Chart is the relative importance of each term, as illustrated graphically by the cumulative bar chart. The scaled estimates listed in the figure are actual regression coefficients for the linear equation formed, though this equation is not used.

Table 4 shows some sample screening results for both sub- and supersonic screening. Often, screening tests confirm a designer's intuition as to which parameters are the important ones. However, some of the variables which turned out to be important would not have been recognized as such without the screening. For example, the area of the horizontal tail (STAIL) is important for the drag due to lift at supersonic speeds. In this case, it is only due to the comparatively large range chosen for this parameter, since tail area, intuitively, should not contribute greatly to drag due to lift. Other variables, however, clearly proved their importance. For example the spanwise location of the kink ( $y_1$ ) was the most contributing parameter for lift induced drag in the subsonic flight regime. This is basically the only reason for having a kink at all: The outboard wing section with low sweep angle is the main producer of lift in subsonic flight whereas in supersonic conditions it only poses a drag penalty. Once the screening results are collected, the actual RSE generation is performed with the just identified most contributing parameters, leaving the others fixed at their nominal values.

**Table 4: Results of Screening Tests:  
The Important Variables**

| Supersonic<br>$k_2$ | Subsonic:<br>$k_2$ | Supersonic<br>$C_{D_o}$ | Subsonic:<br>$C_{D_o}$ |
|---------------------|--------------------|-------------------------|------------------------|
| $S_{tail}$          | $y_1$              | $S_{tail}$              | nal                    |
| $y_1$               | $x_1$              | S                       | $y_1$                  |
| $x_1$               | $x_2$              | tc1                     | $x_1$                  |
| $x_3$               | $x_5$              | $x_5$                   | $x_4$                  |
| $x_5$               | x-wing             | x-wing                  | x-wing                 |
| $C_{Ldesign}$       | $C_{Ldesign}$      | $C_{Ldesign}$           | $C_{Ldesign}$          |
|                     |                    | nay1                    |                        |
|                     |                    | nay2                    |                        |
|                     |                    | nal                     |                        |

With the number of variables now shrunk to a manageable level, a new DOE is set up to generate the data to be used in forming the actual response equations for  $C_{D_o}$  and  $k_2$ . Since drag varies with Mach number which itself varies throughout the mission, it was decided that including Mach number as a variable in the RSE models for drag would add another nonlinearity to the already nonlinear model, thus complicating the fitting process. Therefore, RSEs for  $C_{D_o}$  and  $k_2$  are to be formed for a series of Mach numbers covering the expected operational speed range of the aircraft. Thus, the total drag for a given aircraft configuration was again a function of Mach number and  $C_L$ . So then, following the procedure outlined in Section III, a 5-level Central Composite Design is constructed and the resulting series of simulation runs are executed using the aerodynamic analysis tools listed in Appendix A. The data generated is used to form the second-order polynomial RSEs for each of the two responses in the polar equation at and for the series of operational Mach numbers. A sample listing of the regression coefficients, or the " $b_0$ 's", for one of the RSEs is shown in Figure 9 under the heading "Estimate". These are the actual coefficients which, along with the design variables, make up the RSE of the form of Equation (1). The other three columns contain data concerning the regression accuracy.

## Parameter Estimates

| Term          | Estimate  | Std. Error | t Ratio | Prob> t |
|---------------|-----------|------------|---------|---------|
| Intercept     | -5.878813 | 5.372921   | -1.09   | 0.2891  |
| x1            | 2.3984876 | 2.573549   | 0.93    | 0.3644  |
| x3            | 2.3956492 | 2.503083   | 0.96    | 0.3519  |
| y1            | -0.674068 | 1.963603   | -0.34   | 0.7356  |
| x5            | 1.1983904 | 1.05529    | 1.14    | 0.2719  |
| S-Tail        | -0.000415 | 0.000745   | -0.56   | 0.5846  |
| CLDes         | 8.6087716 | 6.640273   | 1.30    | 0.2121  |
| x1*x1         | -0.933080 | 0.661597   | -1.41   | 0.1765  |
| x3*x1         | 0.4738990 | 0.484103   | 0.98    | 0.3413  |
| x3*x3         | -0.701553 | 0.459443   | -1.53   | 0.1452  |
| y1*x1         | 2.240618  | 0.622419   | 3.60    | 0.0022  |
| y1*x3         | -1.013835 | 0.518682   | -1.95   | 0.0673  |
| y1*y1         | -1.678383 | 0.759487   | -2.21   | 0.0411  |
| x5*x1         | -0.696132 | 0.281092   | -2.48   | 0.0241  |
| x5*x3         | 0.3819572 | 0.234244   | 1.63    | 0.1214  |
| x5*y1         | 0.5088605 | 0.301170   | 1.69    | 0.1094  |
| x5*x5         | -0.257235 | 0.154901   | -1.66   | 0.1151  |
| S-Tail*x1     | 0.0003073 | 0.000249   | 1.23    | 0.2339  |
| S-Tail*x3     | 0.0000541 | 0.000207   | 0.26    | 0.7975  |
| S-Tail*y1     | -0.000355 | 0.000267   | -1.33   | 0.2008  |
| S-Tail*x5     | 0.0000482 | 0.000120   | 0.40    | 0.6940  |
| S-Tail*S-Tail | -1.814e-7 | 1.215e-7   | -1.49   | 0.1538  |
| CLDes*x1      | -1.891504 | 2.178464   | -0.87   | 0.3973  |
| CLDes*x3      | -1.331705 | 1.815387   | -0.73   | 0.4732  |
| CLDes*y1      | 1.7865949 | 2.334069   | 0.77    | 0.4545  |
| CLDes*x5      | -0.481944 | 1.054096   | -0.46   | 0.6533  |
| CLDes*S-Tail  | 0.0002250 | 0.000934   | 0.24    | 0.8124  |
| CLDes*CLDes   | -11.20019 | 9.303713   | -1.20   | 0.2451  |

**Figure 9: Response Surface Equation for  $k_2$  at  $M=2.4$**

There are several ways to validate the accuracy of the RSEs. The first step always is to plot the obtained data. The Whole Model Test in Figure 10 is a plot of the actual response values for  $k_2$  over the predicted values, based on the second order model for the RSE at  $M=2.4$ . The straight line indicates a perfect fit, i.e. all predicted values are equal to the actual for the same levels of input variables. As illustrated in Figure 10, the model predicts the values for  $k_2$  quite well, since all data points are rather close to the straight line. This model fit corresponds to an R-square value of 0.973728. The R-square value is the square of the correlation between the actual and predicted response. Thus, an R-square value of one means that all the errors are zero (i.e. a perfect fit)<sup>10</sup>. The dotted lines indicate the confidence interval for the model, showing a small range with no points falling outside of this range.

The Residual Plot on the right side of Figure 10 is an important verification for the assumption of normality for residuals or statistical error in the response. Hence, the residuals are plotted over predicted values for  $k_2$  based on the assumed model. A "cloud" of data points, indicating no particular pattern, proves the normality assumption for residuals. Hence, there is no reason to suspect violation of the normality assumption for the response  $k_2$ .

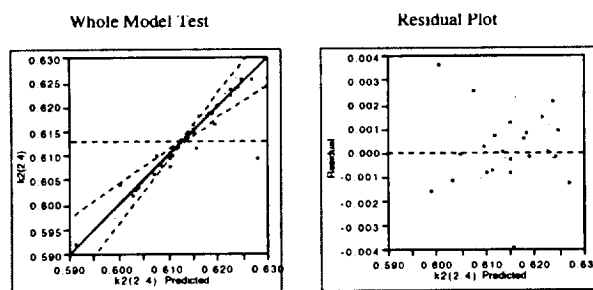


**Figure 10: Whole Model Fit Test- A Validation**

### C. Incorporating the RSE Approximations into the Synthesis Code

FLOPS (FLight OPTimization System) is the code selected to perform the vehicle sizing portion of the design methodology shown in Figure 1. FLOPS, developed by NASA Langley Research Center, is an aircraft sizing code which is used as a multidisciplinary sizing tool to assist the user in his/her conceptual and preliminary design process<sup>16</sup>. FLOPS contains nine modules for aircraft systems analysis: weights, aerodynamics, engine cycle analysis, propulsion data scaling

operational ability to optimize an engine for the four selected cycle variables above. Thus no Response Surface Modeling for propulsion responses was required. Compressor and turbine component maps, which describe the component's off-design performance, are generated externally and provided to FLOPS at run time. Other data such as control laws, correct component map addresses, engine cycle constraints, and engine configuration are provided externally as well.

So then, based on experience gained during the aerodynamic RSE construction and previous supersonic transport concepts, the design variables and their ranges are selected and shown in Table 5. The ranges represent the range spanned by the star points of the CCD. Note that all variables used for this equation are either aerodynamic or propulsion variables. Incorporation of RSEs into the simulation process which capture the effect of structures, manufacturing, and stability/control was not part of this project. It is, however, an interesting and important topic for future research to fully complete the recomposition outlined in Figure 1.

**Table 5: Design Variables for the Aero-Propulsion Optimization**

| Aero / Prop. Variables | Lower Bound | Upper Bound |
|------------------------|-------------|-------------|
| X1                     | 1.54        | 1.62        |
| X3                     | 2.48        | 2.58        |
| Y1                     | 0.50        | 0.58        |
| Root Chord             | 2.19        | 2.35        |
| Surface Area           | 8500 sq. ft | 9500 sq. ft |
| X-wing loc.            | 0.25        | 0.29        |
| Thrust / Weight Ratio  | 0.28        | 0.32        |
| TIT                    | 3000        | 3250        |
| OPR                    | 19          | 21          |
| FPR                    | 3.5         | 4.5         |
| BPR                    | 0.35        | 0.45        |

Figure 12 illustrates the sizing mission which is a split subsonic-supersonic 6500nm profile consistent with the current requirement of subsonic flight over populated land. The stages in Figure 12 are modeled in FLOPS, which then performs a fuel balance to achieve a converged aircraft gross weight.

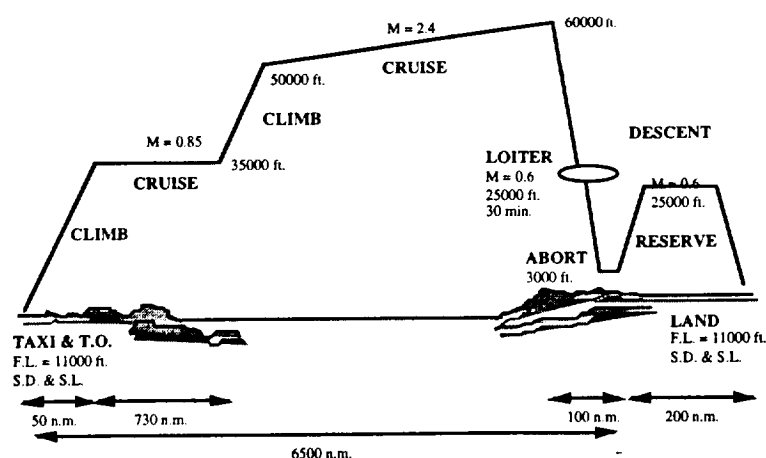


**Figure 12: Typical HSCT Mission**

Using the CCD for the variables and their design ranges depicted in Table 5, the simulation runs are carried out. Through the linear regression approach, a quadratic equation can be

and interpolation, mission performance, takeoff and landing, noise footprint, cost analysis, and program control. However, FLOPS does not model the aerodynamic performance of cranked wing planforms (such as the ones under study here) very well, generally because its routines were tailored to typical subsonic type planforms. This was an additional motivation (besides the increase in aerodynamic analysis fidelity) for replacing the mission drag prediction with the RSEs. FLOPS does give the user the option to insert an externally derived series of polars. Unfortunately, these polars apply only to a single configuration. To analyze a new configuration, a whole new set of polars would have to be generated and inserted manually into the FLOPS input file. This, clearly, makes any attempt of planform optimization difficult. FLOPS does have its own optimization routine, which allows for the variation of aerodynamic shaping variables such as taper, sweep, aspect ratio, and wing area. But for wing shapes such as those seen in Figure 7, variables like aspect ratio (span squared over area) and sweep are not sufficient to uniquely define a cranked, variable sweep planform.

The use of RSM overcomes the limitations of using a single aerodynamics deck for each corresponding configuration. The RSE drag models give the user the ability to optimize a configuration without regenerating aerodynamic decks (for each iteration) by representing the output of the aerodynamic programs with an RSE. It then becomes a simple exercise to evaluate the equation internally to find the new aerodynamic properties for varying flight conditions. In effect, the RSE has captured the essence of a complex external aerodynamics program with a set of equations which can be used as an internal module in FLOPS. This process is depicted below in Figure 11.

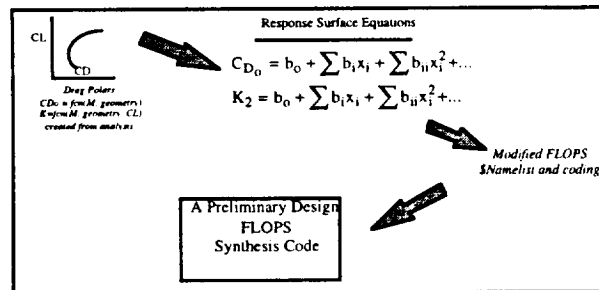


**Figure 11: Incorporating Aerodynamic RSEs into FLOPS**

#### **D. Constrained Aero-Propulsion Optimization**

Once the aerodynamic modeling process is complete, attention turns toward the system level sizing/optimization problem. Revisiting Figure 1, it is seen that once Response Surface Equations for the discipline(s) are formed, the optimization process, given a mission definition, can proceed. Again, a DOE/RSM approach is employed, this time for the purpose of optimizing the system level response, \$/RPM, (as opposed to the modeling function represented by the aerodynamic RSEs) given 11 design variables. After determining variable ranges, a DOE for the generation of simulation results had to be selected. Since eleven is a large number of variables for a Design of Experiments, the Central Composite Design (CCD) was selected to generate the minimum number of data points required to produce a quadratic estimation equation. Use of the fractional factorial CCD with eleven variables at 5 levels requires 151 simulation runs if an additional center point is added and the cube design has Resolution V (see Section III).

FLOPS sizes the engine for the given cycle in order to fly the required HSCT mission. The cycle itself is defined by certain key parameters: the Overall Pressure Ratio (OPR), the Fan Pressure ratio (FPR), the Turbine Inlet Temperature (TIT), and the throttle ratio (TTR). The fan pressure ratios take into account the number of fan stages in order to account correctly for the manufacturing feasibility of the design (i.e. a fan with 2.5 stages would be impossible to manufacture). The engine cycle analysis capability in FLOPS is sufficient for modeling a Mixed Flow TurboFan (such as the one proposed here in the HSCT example) and it contains a fully

established using least square estimators for the parameters. The optimization process is exhibited in Figure 13, displaying the DOE with 151 simulation runs for 11 variables from aerodynamics ( $x_1$ ,  $x_3$ ,  $x_5$ ,  $y_1$ , XWING), propulsion (BPR, FPR, OPR, TIT), and class of the aircraft (T/W, S-wing). These 151 cases represent 151 vehicle sizing problems in which the modified FLOPS code is used to size the vehicle and determine the response, \$/RPM, for each run. This data is then used to form a RSE for \$/RPM as well as the constraints (V-app,  $C_{m\alpha}$ , Flyover and Sideline EPNL, TOFL, and LFL). These polynomials are then brought to a spreadsheet optimizer, where the objective function can be minimized in consideration of the polynomial constraint equations. Hence, the solution found is the constrained point optimal configuration for an HSCT within the design space specified by the ranges of the 11 variables and for the given mission. Finally, a confirmation run to validate results and obtain component weights is performed. These component weights, together with the mission parameters, describe the optimal configuration passed over to the economic uncertainty assessment. The actual execution of this assessment is not part of this report, but has been published under a similar study in Reference 7.

The generation of both the aerodynamic RSEs as well as the just introduced overall objective RSE for \$/RPM was accomplished via UNIX shell scripts, which managed the process of setting up input files, running the specified codes in remote shells, and parsing output files for the required response values. This process automation saved a considerable amount of time over a manual procedure of running hundreds of simulations from the command line.

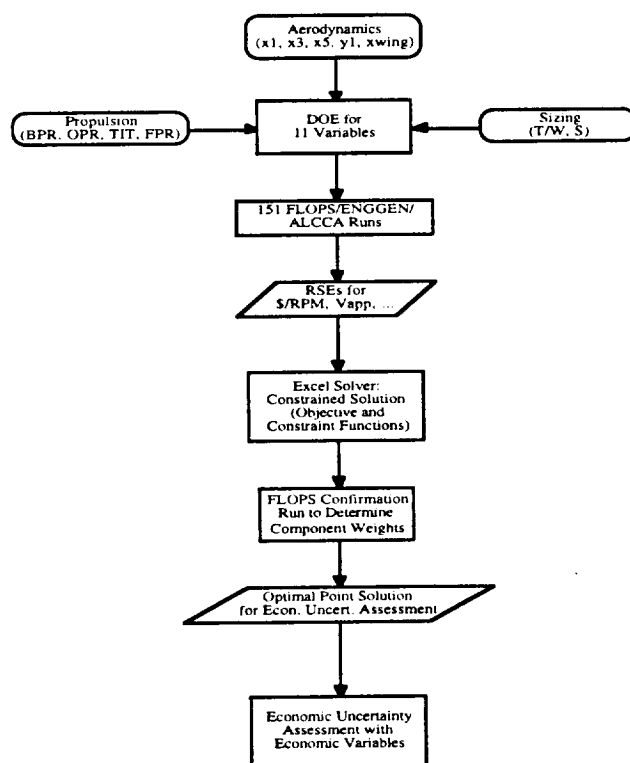


**Figure 13: Design Optimization Approach**

## E. Validation

Figure 14 displays two statistics and their validation. The Summary of Fit lists some characterizations of the least square estimation such as the RSquare (or RSquare Adjusted) value indicating the quality of fit of the data points to the estimated line (See Section III). As mentioned, a value of 1 denotes a perfect fit with all data points lying exactly on the regression line. So then, an R-square of 0.981485 (0.961956) indicates a very good fit for the objective function \$/RPM. The Root Mean Square Error (RSME) is the standard deviation around the mean of the response,



both listed in the Summary of Fit. The low RMSE value of 0.000956 for a mean of 0.152887 attests, just as the RSquare value did, a very good fit of the regression line to the data points. Finally, the number of observations closes the list with the number of data points, entered into the program and used for the statistical analysis.

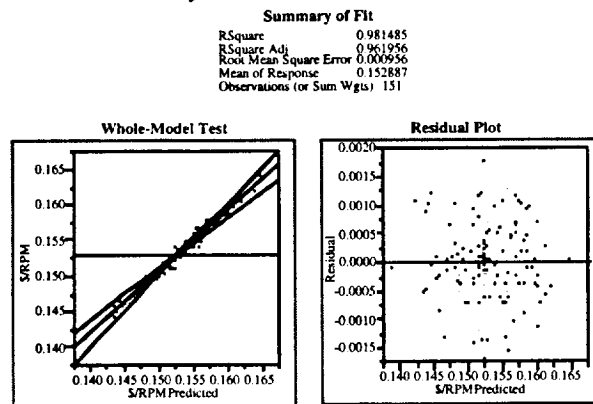


**Figure 14: Summary of Fit and Analysis Validation**

The Whole Model Test plots data of actual  $\$/RPM$  values against the values predicted with the equation, for the same set of inputs. For a perfect fit, all points would be lying on a straight line indicating that the predicted outcome is exactly the same as actually computed by the simulation routine. The Whole Model Test also displays a 95 % prediction interval, denoting that of all predicted outcomes, 95 % of the data points will fall between these two lines. As discussed for the aerodynamic RSE, the Residual Plot shows the residuals (difference of predicted and actual value) of the response ( $\$/RPM$ ) against the predicted values. If this plot shows a pattern or a non-scattered behavior, the normality assumption can usually not be justified. For this analysis, the plot shows a distinct scatter without any pattern, therefore the assumption of normality of the data is accepted and the statistical analysis approved.

The main result of this statistical analysis is now presented in Figure 15. It displays the sensitivities of the objective function ( $\$/RPM$ ) and the constraints (GW, Vapp, TOFL, SLNoise, FONoise, and LFL) with respect to the design variables (T/W, Sref, x-wing, x1, y1, x3, x5, OPR, TIT, FPR, and BPR). These sensitivities indicate the behavior of the response variables with a change in the design variable setting.

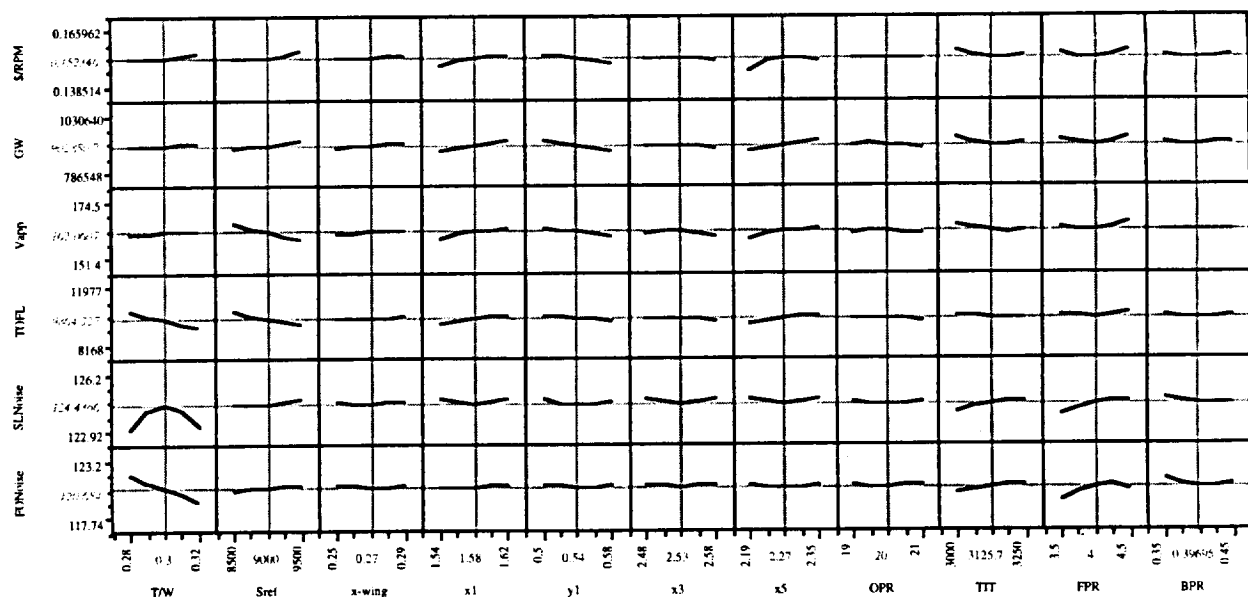


**Figure 15: Response Surface Equation Sensitivities**

The statistical analysis tool used here (JMP<sup>9</sup>) allows a change in the design variable setting with a real time update on the response values (made possible by the simple polynomial evaluation required), giving the designer a feel for the magnitude of the sensitivities. As a result of this sensitivity analysis, it can be seen that T/W has a large effect on noise, while to a lesser degree the planform variables influence the \$/RPM.

The optimization results obtained for this example are summarized in Table 6 and Table 7. Table 6 contains the optimal setting of the design variables while Table 7 lists the minimal value for the objective function, \$/RPM, and the values for the constraints generated by the RSEs as well as the results of a verification run of FLOPS. The right hand column displays the difference of these two values indicating a percentage error for the RSE-based approach. The errors are seen to be modest and acceptable for conceptual/preliminary studies.

**Table 6: Constrained Optimization for Minimum \$/RPM**

| Design Variable | Optimized Value |
|-----------------|-----------------|
| x1              | 1.54            |
| y1              | 0.58            |
| x3              | 2.58            |
| x5              | 2.19            |
| Sref            | 8500            |
| x-wing          | 0.28            |
| T/W             | 0.28            |
| OPR             | 21.00           |
| TIT             | 3148.44         |
| FPR             | 4.50            |
| BPR             | 0.45            |

**Table 7: Constrained Optimization Results**

|                        | RSE     | FLOPS   | % Error |
|------------------------|---------|---------|---------|
| \$/RPM                 | 0.14059 | 0.14347 | -2.00   |
| GW (lbs)               | 804,552 | 831,323 | -3.22   |
| V <sub>app</sub> (kts) | 157.45  | 160.0   | -1.59   |
| TOFL (ft)              | 10,080  | 10,165  | -0.83   |
| LFL (ft)               | 10,107  | 10,271  | -1.59   |
| FONoise, EPNL          | 121.87  | 121.48  | +0.33   |
| SLNoise, EPNL          | 124.78  | 124.31  | +0.38   |

Note that for this optimization the maximum noise levels as specified by FAA FAR 36 were not applied since noise suppression techniques were not modeled in the synthesis code. Hence, the noise constraints are not met during this scheme. The fact that the constraint RSE was formed, however, provides the capability to have a truly noise-constrained vehicle once suppression can be accurately modeled. The optimization yields a wing planform illustrated in Figure 16. The figure on the bottom depicts the planform variable definitions at their optimal settings. It can be seen from the overlay plot on the top that the baseline had a larger span but a smaller sweep in the outer part of the wing than the optimized planform. In addition, with this set of design variables all component weights can be determined and passed through to an economic uncertainty assessment. As mentioned, this exercise is described in Reference 7.



## **Appendix A**

The following public domain tools were used for the aerodynamic analysis: the Boeing Design and Analysis Program (BDAP) for supersonic drag due to lift prediction and skin friction drag, WINGDES for optimum camber and twist, AERO2S for subsonic drag due to lift, and AWAVE for fuselage area ruling. References for these codes appear after the main reference section.

## **References**

1. Sobieszczanski-Sobieski, J., "Multidisciplinary Design Optimization: An Emerging New Engineering Discipline", The World Congress on Optimal Design of Structural Systems, Rio de Janeiro, Brazil, August 1993.
2. Sobieski "A System Approach to Aircraft Optimization" AGARD Structures and Materials Panel 72nd Meeting. Bath, United Kingdom, May, 1991.
3. Dovi, A.R., Wrenn, G.A., Barthelemy, J.F.M., Coen, P., "Multidisciplinary Design Integration System for a Supersonic Transport Aircraft", Presented at the North Atlantic Treaty Organization-AGARD Structures and Materials Panel Meeting, Bath, England, 1-2 May 1991.
4. Malone, B. and W. Mason, "Multidisciplinary Optimization in Aircraft Design Using Analytic Technology Models", *Journal of Aircraft*, Vol. 32 No. 2, March-April 1995.
5. Giunta, A.A., Balabanov, V., Kaufman, M., Burgee, S., Grossman, B., Haftka, R.T., Mason, W.H., and Watson, L.T., "Variable-Complexity Response Surface Design of an HSCT Configuration," in Proceedings of ICASE/LaRC Workshop on Multidisciplinary Design Optimization, Hampton, VA, March, 1995.
6. Englund, W.C., Stanley, D.O., Lepsch, R.A., McMillian, M.M., "Aerodynamic Configuration Design Using Response Surface methodology Analysis," AIAA Aircraft Design, Systems, and Operations Meeting, Monterey, CA, 11-13 August, 1993.
7. Mavris, D. N., Bandte, O., Schrage D.P., "Economic Uncertainty Assessment of an HSCT using a Combined Design of Experiments / Monte Carlo Approach," 17th Annual Conference of the ISPA, San Diego, CA, May 1995.
8. Box, G.E.P., Draper, N.R.; *Empirical Model-Building and Response Surfaces*; John Wiley & Sons, Inc.; New York; 1987.
9. Box, G.E.P., Hunter, W.G., Hunter, J.S., Statistics for Experimenters, John Wiley & Sons, Inc., New York, 1978.
10. SAS Institute Inc., *JMP Computer Program and User's Manual*, Cary, NC, 1994.
11. Dieter, G.E., Engineering Design, A Materials and Processing Approach, 2nd Edition, McGraw Hill Inc., New York, NY, 1971.
12. Montgomery, D.C., Design and Analysis of Experiments, John Wiley & Sons, Inc., New York, 1991.
13. Swan, W. "Design Evolution of the Boeing 2707-300 Supersonic Transport". Boeing Commercial Airplane Company, No Date Available.
14. Sakata, I.F., and Davis, G.W., "Evaluation of Structural Design Concepts for Arrow-Wing Supersonic Cruise Aircraft," NASA CR-2667, May, 1977.

15. Carlson, H.W., Darden, C.M., Mann, M.J., "Validation of a Computer Code for Analysis of Subsonic Aerodynamic Performance of Wings with Flaps in Combination with a Canard or Horizontal Tail and a Application to Optimization," (AERO2S), NASA-TP-2961, 1990.
16. McCullers, L.A. *Flight Optimization System User's Guide*, Version 5.7, NASA Langley Research Center, 1995.

## APPENDIX A REFERENCES

- A.1 "AWAVE User's Guide for the Revised Wave Drag Analysis Program, NASA Langley Research Center, September, 1992.
- A.2 "WINGDES", Carlson, H.W., Walkley, K.B., "Numerical Methods and a Computer Program for Subsonic and Supersonic Aerodynamic Design and Analysis of Wings with Attainable Thrust Considerations", NASA-CR-3803, 1984.
- A.3 BDAP- Middleton, W.D., Lundry, J.L., "A System for Aerodynamic Design and Analysis of Supersonic Aircraft," NASA-CR-3351, 1980.